Published April 17, 2006

Direct in vivo monitoring of sarcoplasmic reticulum Ca^{2+} and cytosolic cAMP dynamics in mouse skeletal muscle

Rüdiger Rudolf,[1,2] Paulo J. Magalhães,[1] and Tullio Pozzan[1,2]

[1]Department of Biomedical Sciences, University of Padua, I-35121 Padua, Italy
[2]Venetian Institute of Molecular Medicine, I-35129 Padua, Italy

Skeletal muscle contraction depends on the release of Ca^{2+} from the sarcoplasmic reticulum (SR), but the dynamics of the SR free Ca^{2+} concentration ($[Ca^{2+}]_{SR}$), its modulation by physiological stimuli such as catecholamines, and the concomitant changes in cAMP handling have never been directly determined. We used two-photon microscopy imaging of GFP-based probes expressed in mouse skeletal muscles to monitor, for the first time in a live animal, the dynamics of $[Ca^{2+}]_{SR}$ and cAMP. Our data, which were obtained in highly physiological conditions, suggest that free $[Ca^{2+}]_{SR}$ decreases by ~50 μM during single twitches elicited through nerve stimulation. We also demonstrate that cAMP levels rise upon β-adrenergic stimulation, leading to an increased efficacy of the Ca^{2+} release/reuptake cycle during motor nerve stimulation.

Introduction

Excitation–contraction coupling in skeletal muscle depends on motor neuron–induced cell depolarization and the subsequent interaction between the dihydropyridine receptor (DHPR) and the ryanodine receptor (RYR), resulting in the release of Ca^{2+} from the terminal cisternae of the sarcoplasmic reticulum (SR). Although much has been done in this field, studies of the quantitative aspects and kinetics of the concentration of free Ca^{2+} in the SR lumen ($[Ca^{2+}]_{SR}$) have been marred by technical challenges. Most of the available data come from biochemical studies on isolated fractions (Volpe and Simon, 1991), x-ray microanalysis studies on rapidly frozen samples (Somlyo et al., 1981), or extrapolations measuring the rise of cytosolic $[Ca^{2+}]$ ($[Ca^{2+}]_c$; Baylor and Hollingworth, 2003). Recently, direct monitoring of $[Ca^{2+}]_{SR}$ made use of the fluorescent dyes fluo-5N (Kabbara and Allen, 2001) or mag-indo-1 (Launikonis et al., 2005) in isolated frog muscle fibers. These approaches still suffer from major drawbacks; the subcellular localization of the dyes is not SR specific, they are difficult to apply to live animals, and, thus far, no $[Ca^{2+}]_{SR}$ kinetics during excitation–contraction coupling with high temporal resolution have been determined. Cameleon Ca^{2+} sensors potentially overcome most of these problems. First, as they are genetically encoded, they can be selectively targeted to subcellular compartments. Second, their ratiometric nature ensures that changes in probe quantity and movement artifacts are inherently corrected (Rudolf et al., 2004). Third, they can be introduced into intact tissues and organisms by standard techniques (Rudolf et al., 2004). Finally, the recent molecular engineering of cameleons have functionally silenced the two central domains (i.e., CaM and the M13 peptide), rendering these probes virtually inert as cellular signaling molecules while maintaining their Ca^{2+}-sensing properties (Palmer et al., 2004).

Using an SR-targeted cameleon and two-photon confocal microscopy in live mouse, we have addressed two unsolved issues in muscle physiology: (1) direct quantitative measurement of the kinetics and amplitude of $[Ca^{2+}]_{SR}$ transients during single twitches and tetanic stimulation, and (2) the effect of β-adrenergic stimulation on SR Ca^{2+} handling. It is known that the force of contraction can be enhanced by β-receptor agonists in both heart and skeletal muscle (Cairns and Dulhunty, 1993b). In cardiac muscle, it involves PKA-dependent phosphorylation of troponin I (Zhang et al., 1995), DHPR (Bean et al., 1984), phospholamban (Lindemann et al., 1983), and RYR II (Yoshida et al., 1992). In skeletal muscle, the mechanism is less studied, but, as in the heart, it seems to rely on PKA-dependent phosphorylation of different targets, such as DHPR (Sculptoreanu et al., 1993) and RYR I (Sonnleitner et al., 1997). Regarding RYR I in particular, it is still a matter

Correspondence to Rüdiger Rudolf: ruediger.rudolf@itg.fzk.de

Abbreviations used in this paper: CPA, cyclopiazonic acid; DHPR, dihydropyridine receptor; K_d, apparent dissociation constant; PB, phosphate buffer; PKA, protein kinase A; RYR, ryanodine receptor; SERCA, sarcoendoplasmic reticulum Ca^{2+} ATPase; ROI, regions of interest; SR, sarcoplasmic reticulum; TA, tibialis anterior.

The online version of this article contains supplemental material.

Supplemental Material can be found at:
/content/suppl/2006/04/17/jcb.200601160.DC1.html

The Journal of Cell Biology, Vol. 173, No. 2, April 24, 2006 187–193
http://www.jcb.org/cgi/doi/10.1083/jcb.200601160

Published April 17, 2006

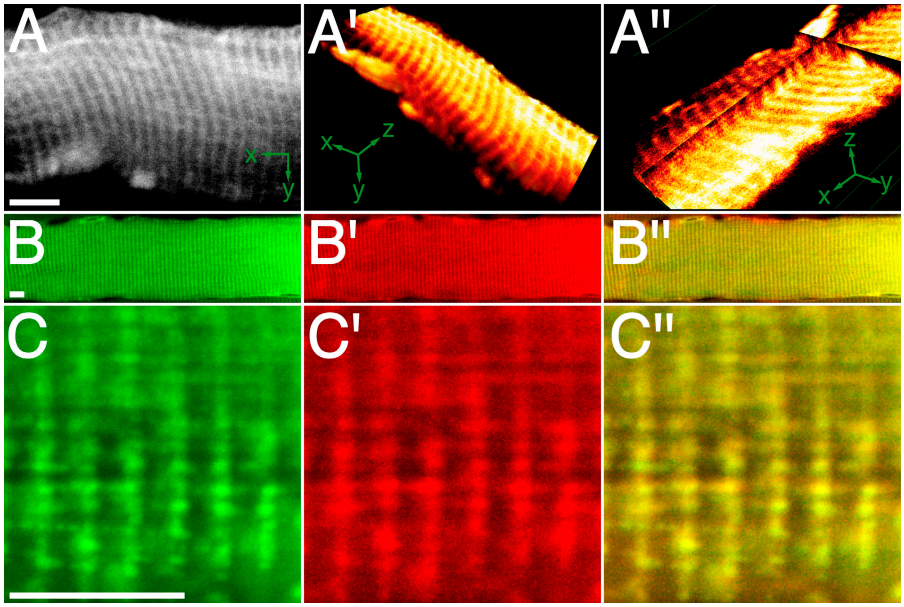

Figure 1. **D1ER is localized in the SR.** TA muscle was transfected with cDNA encoding D1ER. 2 wk later, optical sections were made in situ with two-photon microscopy (A–A″) or with confocal microscopy on longitudinal cryosections immunostained for SERCA 1 (B–C″). (A) Optical section of a single fiber (x-y orientation as indicated). (A′) 3D reconstruction of the fiber. (A″) Multiplanar reconstruction showing the optical plane in A as basal plate and the fluorescence signals in the z-dimension along the cross-shaped sheer plan (x-y-z orientation as indicated). A′ and A″ were made with OsiriX software. (B–C″) Fluorescence signals of D1ER (B and C, green), SERCA 1 immunostaining (B′ and C′, red), and overlay (B″ and C″, yellow). Bars, 10 μm.

of discussion whether phosphorylation of the channel is physiologically relevant (Sonnleitner et al., 1997; Blazev et al., 2001).

We demonstrate not only that a massive decrease of $[Ca^{2+}]_{SR}$ occurs during tetanic stimulation in vivo, but also that a substantial drop is elicited even during single muscle twitches. Using Epac1–cAMP sensor (Nikolaev et al., 2004), we show the first dynamic measurement of [cAMP] in a live animal and provide direct evidence that during β-adrenergic force potentiation the $[Ca^{2+}]_{SR}$ at rest, as well as the SR Ca^{2+} efflux and reuptake, are markedly increased.

Results and discussion

Expression of YC6.2ER and D1ER

Tibialis anterior (TA) muscles were transfected in vivo with cDNA encoding YC6.2ER or D1ER, which was targeted to the SR, as previously described (Rudolf et al., 2004). As shown in Fig. 1 (A–C″) for D1ER, the probe exhibited the typical striation pattern for SR. This pattern was always observed for D1ER, whereas YC6.2ER showed a more diffuse staining when strongly overexpressed. Data obtained with YC6.2ER was similar to that with D1ER; given the precise localization pattern of D1ER, however, only data with this probe is included in our study. Fig. 1 (B–C″) depicts confocal images of longitudinal slices of muscles transfected with D1ER (Fig. 1, B and C, green) and immunostained against sarcoendoplasmic reticulum Ca^{2+}-ATPase (SERCA) type 1 (Fig. 1, B′ and C′, red). The overlay shows the colocalization of the two proteins (Fig. 1, B″ and C″). This colocalization, along with the functional data revealing a drop in $[Ca^{2+}]_{SR}$ upon stimulation (see the following section), shows that D1ER is correctly targeted when expressed in live mouse skeletal muscle.

Strong $[Ca^{2+}]_{SR}$ decrease upon single twitch contraction

To quantify the drop of $[Ca^{2+}]_{SR}$ upon contraction, we studied the probe response at a stimulation frequency of 1 Hz. The background-subtracted YFP/CFP ratio images were scanned along the fiber length in 10-ms windows; in parallel, fiber deflection was measured as an indicator of muscle contraction (Fig. 2 A). The fibers exhibited a twitch profile of ∼100 ms in duration, which is typical of fast-twitch fibers and is as expected for this muscle. The ratio changes followed almost exactly the kinetics of fiber deflection, with the drop in ratio clearly preceding muscle contraction. However, the nadir in $[Ca^{2+}]_{SR}$, as measured with D1ER, is reached ∼30 ms after the start of contraction, which is similar to the time course of $[Ca^{2+}]_c$ rises that was previously measured (Rudolf et al., 2004), but definitively slower than the time-to-peak level in $[Ca^{2+}]_c$ as measured with a fast Ca^{2+} indicator (Baylor and Hollingworth, 2003). This discrepancy may be attributable to a variety of factors. First, a relatively slow dissociation of Ca^{2+} and conformational change of the cameleon may lead to a delay between the actual drop in $[Ca^{2+}]_{SR}$ and the decrease in fluorescence resonance energy transfer. We do not consider this possibility very likely because, according to fast kinetics measurements in vitro (Palmer et al., 2004), the dissociation rate constant (k_{off}) of D1ER is 256 s^{-1} and, thus, the indicator should be able to monitor a faster drop if it occurred; indeed, we calculated an even higher apparent dissociation constant (K_d) in HeLa cells than the one previously determined in vitro (Fig. S1, available at http://www.jcb.org/cgi/content/full/jcb.200601160/DC1), but the k_{off} could not be measured in situ. Second, the signal reflects the mean of the whole SR, as it is localized not only in the terminal cisternae but also, as suggested by the colocalization of the probe with SERCA 1 (Fig. 1, B″ and C″), in the longitudinal SR; in the latter, the changes in $[Ca^{2+}]_{SR}$ may be smaller and delayed. Third, the kinetics shown may reflect the actual situation, indicating that a decrease of $[Ca^{2+}]_{SR}$ may also continue during the decay phase of $[Ca^{2+}]_c$.

The maximal drops in absolute YFP/CFP ratio from the baseline differed considerably between different analyzed fibers, ranging from ∼3–25% of the initial value. The calibration

Published April 17, 2006

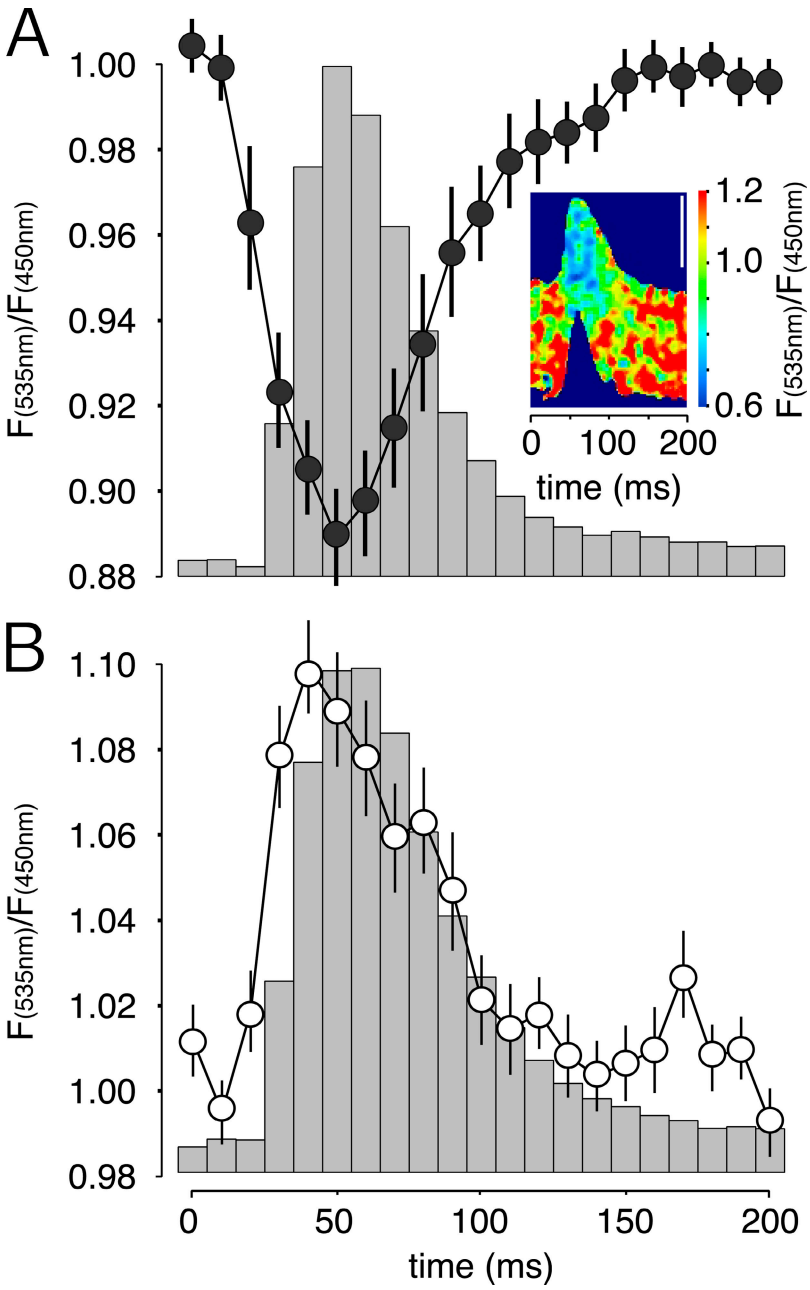

Figure 2. **D1ER reveals transient decreases of $[Ca^{2+}]_{SR}$ during single twitches in situ.** TA muscle was transfected with cDNA encoding D1ER (A) or YC2 (B). Fluorescence signals were monitored in situ during contraction, and the stimulation frequency was 1 Hz. Graphs show $[Ca^{2+}]_{SR}$ (A) or $[Ca^{2+}]_c$ (B) transients as measured by decrease or increase, respectively, of the YFP/CFP ratio normalized to the values in the relaxed state. Data are mean ± SEM. $n = 5$ fibers. 15 twitches per fiber were averaged. The contraction profile corresponding to the Ca^{2+} transients is indicated by the columns. The inset image in A shows a D1ER-expressing muscle fiber during contraction, with the YFP/CFP ratio indicated by pseudocolors (color scale, right). Bar, 50 μm.

of ratio signals into absolute $[Ca^{2+}]$ was derived from in situ measurements in culture cells (Fig. S1). Based on the known properties of D1ER and assuming a 200-μM K_d for Ca^{2+} within the SR lumen (which is higher than that calculated in vitro; Fig. S1), the basal $[Ca^{2+}]_{SR}$ was 308 ± 30 μM and exhibited a drop during single twitches of 53 ± 6 μM (for both, mean ± SEM; $n = 18$ fibers).

Effects of the partial inhibition of the SERCA

We then tested the effect of partial inhibition of the SERCA, using an appropriate dose of cyclopiazonic acid (CPA) to verify the importance of the SERCA on the kinetics of $[Ca^{2+}]_{SR}$ changes during stimulation. Intramuscular injection of CPA (100 μl of 100 μM CPA) caused a time-dependent drop of YFP/CFP ratio that typically stabilized ∼30–40 min after application of the drug at a value of 1.87 ± 0.17 (mean ± SEM; $n = 3$ fibers), corresponding to ∼134 μM. Under these conditions, SERCA inhibition was only partial; we could repetitively induce fiber contraction (Fig. 3 A), whereas, as shown in skinned rat fibers, a muscle fiber may contract only few times after complete block of the SERCA (Posterino and Lamb, 2003). Indeed, nerve stimulation of fibers treated with this CPA concentration revealed an amplification of contraction intensity (Fig. 3 A), albeit the resting $[Ca^{2+}]_{SR}$ was significantly lower than in controls and the maximal level of $[Ca^{2+}]_{SR}$ decrease was reduced (Fig. 3 B, top). In parallel experiments, we confirmed that the peak level in $[Ca^{2+}]_c$, as measured with cameleon YC2, is increased by this CPA treatment (unpublished data). Fiber contractions upon a single nerve impulse in the presence of CPA (Fig. 3 B)

Published April 17, 2006

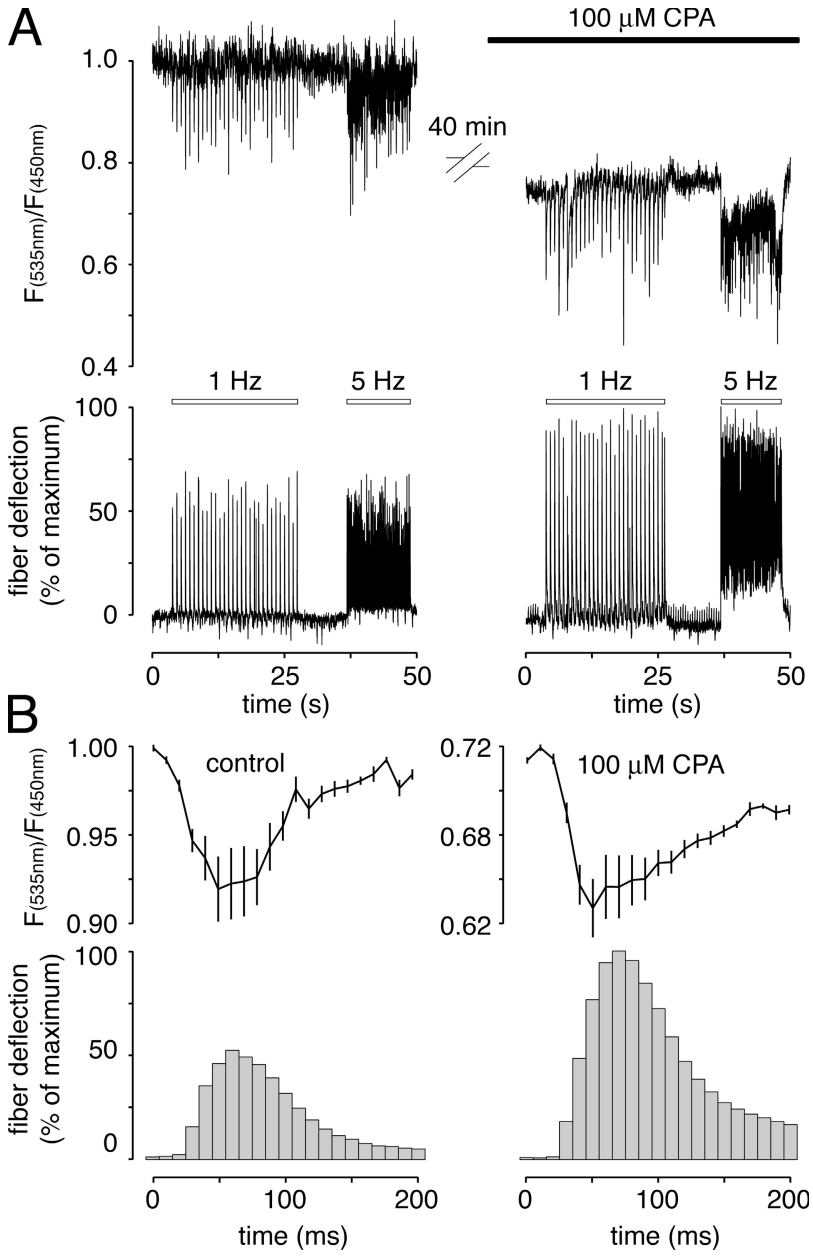

Figure 3. **Effects of partial inhibition of the SERCA.** Conditions were as in Fig. 1. (A) YFP/CFP ratio (top) and contraction profile (bottom) of a single experiment, with stimulation frequencies of 1 or 5 Hz and injection of CPA as indicated. Values are normalized to the start of the experiment. (B, top) $[Ca^{2+}]_{SR}$ transients for control fibers and fibers treated with 100 μM CPA, as indicated. (bottom) The corresponding contraction profiles. Stimulation frequency was 1 Hz. For each experiment and condition, 25 individual twitches were averaged. Data shown represent mean ± SEM. $n = 4$ fibers. Values are normalized to control.

were also stronger than in control conditions; similar results have been obtained in another study (Rios and Stern, 1997). This cannot be easily explained if all Ca^{2+} release from the SR was caused by electromechanical coupling, i.e., if it occurred only during the action potential. In this case, one would expect the contraction and rise in $[Ca^{2+}]_c$ to be the same, or smaller, in CPA-treated muscle compared with controls. Several possibilities, which are not mutually exclusive, may be suggested: (1) a reduced cytoplasmic Ca^{2+} buffering in the presence of CPA, caused by a slight increase in $[Ca^{2+}]_c$ (with partial saturation of $[Ca^{2+}]_c$ buffers); a small capacitative Ca^{2+} entry might be activated under these experimental conditions (Kurebayashi and Ogawa, 2001); however, we found no significant increase in basal $[Ca^{2+}]_c$ in the presence of CPA (unpublished data); (2) a reduced contribution of the Ca^{2+}-binding activity of the SERCA, given that SERCA bound to CPA are in a low Ca^{2+} affinity conformation (Goeger and Riley, 1989); and (3) that the massive release caused by electromechanical coupling was followed by a small, but prolonged, release of Ca^{2+} (apparently, as monitored with D1ER), which is possibly a consequence of Ca^{2+}-induced Ca^{2+} release. A slow release could be partially counteracted by the SERCA activity and, thus, be unmasked in fibers treated with CPA. The role and existence of Ca^{2+}-induced Ca^{2+} release in fast skeletal muscle is surely of minor relevance (Shirokova et al., 1996, 1998; Rios and Stern, 1997), but to our knowledge it has never been completely excluded.

Ca^{2+} release from the SR upon β-adrenergic potentiation in situ

Our experimental setup enabled us to address an unanswered question of the utmost biological relevance: the role of the SR in β-adrenergic force potentiation. First, we directly studied the

Published April 17, 2006

effect of isoproterenol, which is a β−adrenergic agonist, on [cAMP] by transfecting TA muscles with Epac1–cAMP sensor (Nikolaev et al., 2004). The subcellular distribution of fluorescence was homogeneous (cytoplasmic) within the fibers (Fig. 4 A). We found a highly reproducible rise in [cAMP] upon injection of isoproterenol, as shown by the increase of the CFP/YFP ratio to 1.33 ± 0.03 (mean ± SEM; $n = 8$ fibers; data normalized to control; Fig. 4 B). The rise was already maximal 10 min after application of the drug and decreased slightly thereafter (Fig. 4 B). Similar results were obtained with another fluorescent PKA-based cAMP probe (Zaccolo and Pozzan, 2002) and upon injection of high doses of forskolin (250 μM); given the probe's ∼2-μM cAMP K_d (Nikolaev et al., 2004), the rise in [cAMP] that is attributable to β-adrenergic stimulation is likely in the micromolar range.

As shown in Fig. 4 C (bottom), the application of isoproterenol also led to a larger fiber deflection, which is indicative of the expected force potentiation. This increase in single-twitch amplitude was paralleled by four interesting phenomena. First, the basal-normalized YFP/CFP ratio increased from 1.00 ± 0.02% to 1.06 ± 0.01% (mean ± SEM; $n = 3$ fibers) after injection of isoproterenol (Fig. 4 C, top). According to the calibration procedure described in the supplemental material, this would account for a rise in $[Ca^{2+}]_{SR}$ from ∼278 to ∼311 μM. Second, the decrease of YFP/CFP ratio during single twitches was enhanced in the presence of isoproterenol without interim stimulation (Fig. 4 C, top), accounting for drops in $[Ca^{2+}]_{SR}$ of ∼65 and ∼99 μM in the absence and presence of isoproterenol, respectively; this effect was even stronger upon 50 Hz stimulation, where the corresponding changes were calculated to be ∼83 and ∼153 μM. Third, the kinetics of the Ca^{2+}-release/reuptake cycle during single twitches in the presence of isoproterenol had the same duration as in controls (160 ms). Thus, the rise in [cAMP], presumably via PKA-dependent phosphorylation, increases Ca^{2+} release from the SR, but does not change the kinetics of release/reuptake. Finally, although the drop in $[Ca^{2+}]_{SR}$ was higher in the presence of isoproterenol, the time constants from peak to half-maximal recovery were virtually identical in the absence (35 ms) and presence (36 ms) of the adrenergic stimulus. Thus, during the same time period more Ca^{2+} is taken up by the SR in fibers stimulated by isoproterenol compared with controls.

In summary, the data presented show that stimulation of β-adrenergic receptors in skeletal muscles leads to a major and prolonged rise of [cAMP] accompanied by an increase of basal $[Ca^{2+}]_{SR}$ and a drop in $[Ca^{2+}]_{SR}$ during contraction. The increased fiber contraction is clearly dependent on the larger Ca^{2+} release because previous work has shown that, unlike in cardiac fibers, cAMP-dependent PKA activation does not modify the Ca^{2+} sensitivity of the contractile apparatus (Fabiato and Fabiato, 1978; Cairns and Dulhunty, 1993a). In particular, only myosin-binding protein C and troponin I of cardiac muscle may be phosphorylated by PKA (Tong et al., 2004).

Regarding the effect of isoproterenol on Ca^{2+} release, different, nonmutually exclusive explanations may be considered. First, a higher basal $[Ca^{2+}]_{SR}$ might account for a larger release of Ca^{2+} during contraction. However, no correlation between

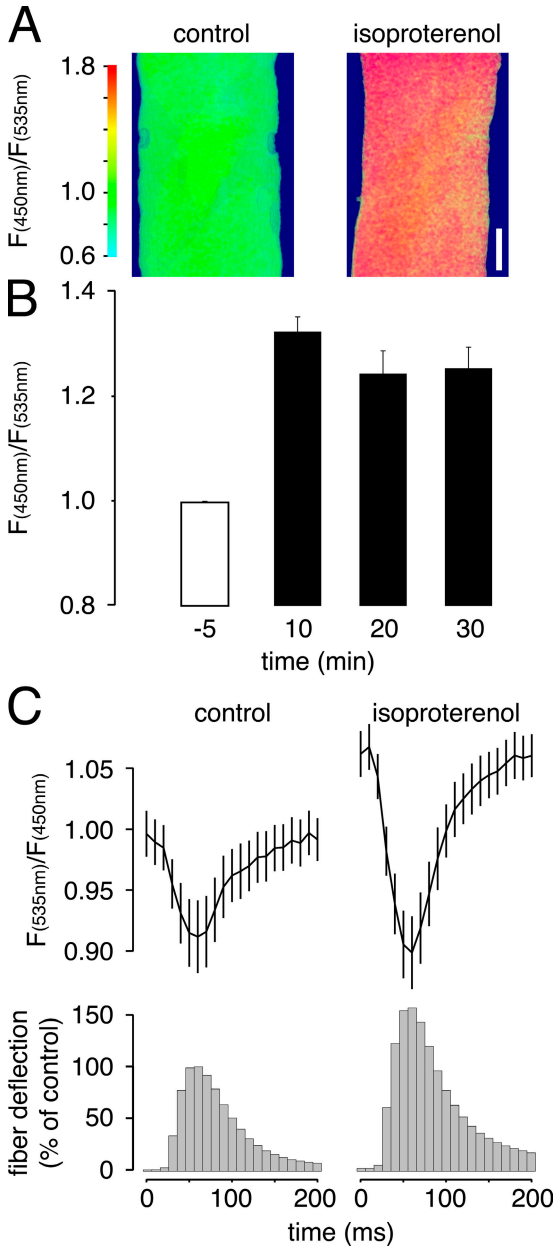

Figure 4. **In situ β-adrenergic potentiation involves rise of [cAMP] and amplification of Ca^{2+} release and reuptake from the SR.** TA muscle was transfected with cDNA coding for Epac1–cAMP sensor (A and B) or D1ER (C), fluorescence signals were monitored in situ. (A) Epac1–cAMP sensor–expressing fiber before (left) and 10 min after (right) injection of isoproterenol; the CFP/YFP ratio is indicated by pseudocolors (color scale, left). Bar, 10 μm. (B) Epac1–cAMP sensor response to isoproterenol. Data shown represent mean ± SEM. $n = 8$ fibers. Values are normalized to control and the time from injection is as indicated. (C) Stimulation frequency was 1 Hz. (top) $[Ca^{2+}]_{SR}$ transients of the same fibers before (control) and after (isoproterenol) treatment with isoproterenol. (bottom) Corresponding contraction profiles. For each experiment and condition, 25 individual twitches were averaged. Data shown represent mean ± SEM. $n = 3$ fibers. Values are normalized to control.

basal $[Ca^{2+}]_{SR}$ and the drop during contraction was observed; neither by ourselves (Fig. S2, B and C, available at http://www.jcb.org/cgi/content/full/jcb.200601160/DC1) nor in a previous study (Posterino and Lamb, 2003). Second, the increased Ca^{2+} efflux could be attributable to direct cAMP/PKA-dependent

Published April 17, 2006

activation of RYR I; this possibility has been previously proposed (Sonnleitner et al., 1997; Blazev et al., 2001), but no convincing evidence has been provided. Third, and most likely, it could be caused by PKA-dependent phosphorylation of DHPR that increases its coupling to RYR I. Strong evidence supporting this mechanism has been obtained in myoblasts (Sculptoreanu et al., 1993).

The effect of β-adrenergic stimulation on Ca^{2+} accumulation was unexpected for fast skeletal muscle, which is known to be devoid of phospholamban (Vangheluwe et al., 2005). Evidence supporting a role for cAMP in SERCA stimulation has been described in the skinned fibers of cat (Fabiato and Fabiato, 1978), but this finding has been neglected for almost 30 yr. A simple, conservative explanation may be an indirect effect of cAMP/PKA on SERCA activity, mediated by PKA activation of glycogen metabolism (Gross et al., 1976); both pyruvate (Hermann et al., 2000) and local ATP generation by SR-bound glycolytic enzymes appear particularly important for the activity of SERCA (Korge and Campbell, 1994). Increased availability of glucose (and, thus, ATP) may explain the higher Ca^{2+} loading of the SR upon β-adrenergic stimulation.

Materials and methods

Expression plasmids, antibodies, and chemicals
Transfection experiments used the following constructs in pcDNA3 (Invitrogen): YC2, D1ER, and Epac1–cAMP sensor were gifts from R.Y. Tsien (University of California, San Diego, San Diego, CA) and M.J. Lohse (University of Würzburg, Würzburg, Germany). The A23187, ascorbic acid, CPA, digitonin, histamine, isoproterenol, and thapsigargin (all from Sigma-Aldrich) used were of the highest available grade. All injected drugs and cDNAs were diluted in sterile physiological solution (0.9% NaCl). SERCA 1 antibody (clone VE121G9) was purchased from Affinity BioReagents and Alexa Fluor 568 goat anti–mouse IgG was purchased from Invitrogen.

Animals
All experiments used C57BL/10 mice (aged 6–12 mo; Charles River Italia). Animal handling was approved by the local authority for veterinary services, in accordance with Italian law. For anesthesia, Rompun (Bayer) and Zoletil 100 (Laboratoires Virbac) were injected i.p.

Transfection
Transfection was carried out using an electroporation-based method of the TA muscle, as previously described (Rudolf et al., 2004).

Slice preparation and immunohistochemistry
For immunostaining, muscles were first stretched, fixed overnight at 4°C in 4% paraformaldehyde in 0.1 M phosphate buffer (PB), and dehydrated in 10% sucrose/PB; they were then snap frozen in liquid nitrogen–cooled isopentane. The muscle was embedded in Jung tissue-freezing medium and 10-μm-thick cryosections were prepared using a cryostat (model CM1850; Leica). After drying, the sections were quenched with 50 mM NH_4Cl/PB and permeabilized with 0.1% Triton X-100/PB. Sections were then rinsed with PB, blocked with 0.2% gelatin/PB and incubated with anti-SERCA 1 antibody (1:500, diluted in 0.2% gelatin/PB) overnight at 4°C. Sections were blocked again with 0.2% gelatin/PB and incubated with the secondary antibody (1:250, diluted in 0.2% gelatin/PB) for 2 h. Finally, the preparations were rinsed in 0.2% gelatin/PB and PB and mounted in Mowiol.

Confocal analysis of immunostainings
Confocal images of immunostained sections were obtained with a microscope (Radiance 2100MP; BioRad Laboratories) equipped with an Ar (488-nm line) laser and a HeNe laser (543-nm line), a 60×/1.4 NA objective (Nikon), a 560DCLPXR dichroic mirror, HQ515/30 and E570LP emission filters (Chroma Technology Corp.) for the detection of cameleon, and Alexa Fluor 568 fluorescence signals. Images were taken at 1,024 × 1,024 pixel resolution and 50 lines s^{-1} scan speed.

In vivo two-photon microscopy
This procedure was performed as previously described (Rudolf et al., 2004), with minor modifications. Unless otherwise indicated, video microscopy was performed at 256 × 256 pixels with a 1.95-Hz acquisition frequency. For $[Ca^{2+}]_{SR}$ studies, images were acquired at 1,024 × 1,024 pixels at 166 lines s^{-1}. Drug injection (1 mM CPA, 100 μM CPA, or 10 μM isoproterenol + 1 mM ascorbic acid) was performed locally using a 30-gauge needle (Artsana) with a typical volume of 100 μl. To allow the muscle to recover from the injection-induced swelling, microscopic observation was interrupted for at least 5 min.

Data analysis of ratiometric images
Datasets were analyzed essentially as previously described (Rudolf et al., 2004), using ImageJ software (National Institutes of Health). Fibers were oriented in the microscopic field with the longitudinal axis perpendicular to the line scan direction, matching the timeline to the long fiber axis. A mask containing the whole observed part of the fiber was created from the corresponding median-filtered YFP video by intensity thresholding. Next, both CFP and YFP videos were mean filtered (1 pixel kernel) to suppress hot pixel noise, background intensity was subtracted when necessary, and the mask was applied. For the data shown in Fig. S1, the mean CFP and YFP values were determined inside the mask region; subsequent calculations and graphs used Excel 2002 (Microsoft). Ratio plots were normalized using the last 10 images preceding the first contraction as reference values. The ratio values during single twitches, such as in Figs. 2–4, were obtained as follows. A YFP/CFP ratio video was created by applying the custom-made ImageJ plug-in Ratio Plus. Ratio values were then determined along the fiber length in regions of interest (ROIs) with a width of 5 pixels, equaling 10-ms time frames. The background value at any ROI was calculated as the mean at that position in the 10 frames preceding the first contraction and was subtracted from the ROIs obtained during contraction using the formula: $n_{i+a} = (x_{i+a} + m - m_a)/m_c$, where n_{i+a} is the normalized ratio value at point i + a, x_{i+a} is the measured ratio value at point i + a, m is the mean ratio value along the whole fiber length, and m_a is the mean ratio value at point a. In Fig. 2, m_c is equal to m, whereas in Figs. 3 and 4 it is equal to m of the corresponding controls. In parallel, the relative fiber deflection was determined using the last frame before the first contraction as a blank. For the average calculations shown in Figs. 2–4, individual twitches were synchronized by setting the first ROI with deflection as the start of contraction. For the timelines shown in Fig. 3 A, subsequent frames were treated as continuous in time; this assumption is valid because the time-lapse between the last scan line of an image and the first one of the following frame was of the same order as the jump from one line to the next in the same frame, and because contractions that initiated in one frame and continued in a following frame, appeared smooth in procedure after recomposition, as executed in Fig. 3 A.

Online supplemental material
Experiments showing the functionality and correction for movement artifacts of D1ER as well as a detailed description of D1ER in situ calibration are available online. Online supplemental material is available at http://www.jcb.org/cgi/content/full/jcb.200601160/DC1.

We thank Drs. M. Ikura, M.J. Lohse, RY. Tsien, and M. Brini for their generous gifts of plasmids and antibodies, and Drs. M. Mongillo, M. Zaccolo, D. Sandonà, E. Damiani, and A. Margreth for fruitful discussions.

R. Rudolf was supported by grants from the University of Padua and the Deutsche Forschungsgemeinschaft (RU 923/1-1). The following grants to T. Pozzan also partially supported this work: Italian Telethon (grant 1226), Italian Association for Cancer Research, Italian Ministry of Universities (Special Projects Prin RBNE01ERXR-001 and 20033054449-001, and FIRB 2002053318-005), Italian Ministry of Health, and the CARIPARO foundation.

Submitted: 27 January 2006
Accepted: 16 March 2006

References

Baylor, S.M., and S. Hollingworth. 2003. Sarcoplasmic reticulum calcium release compared in slow-twitch and fast-twitch fibres of mouse muscle. *J. Physiol.* 551:125–138.

Bean, B.P., M.C. Nowycky, and R.W. Tsien. 1984. Beta-adrenergic modulation of calcium channels in frog ventricular heart cells. *Nature*. 307:371–375.

Blazev, R., M. Hussain, A.J. Bakker, S.I. Head, and G.D. Lamb. 2001. Effects of the PKA inhibitor H-89 on excitation-contraction coupling in skinned and intact skeletal muscle fibres. *J. Muscle Res. Cell Motil.* 22:277–286.

Cairns, S.P., and A.F. Dulhunty. 1993a. Beta-adrenergic potentiation of E-C coupling increases force in rat skeletal muscle. *Muscle Nerve*. 16:1317–1325.

Cairns, S.P., and A.F. Dulhunty. 1993b. The effects of beta-adrenoceptor activation on contraction in isolated fast- and slow-twitch skeletal muscle fibres of the rat. *Br. J. Pharmacol.* 110:1133–1141.

Fabiato, A., and F. Fabiato. 1978. Cyclic AMP-induced enhancement of calcium accumulation by the sarcoplasmic reticulum with no modification of the sensitivity of the myofilaments to calcium in skinned fibres from a yeast skeletal muscle. *Biochim. Biophys. Acta*. 539:253–260.

Goeger, D.E., and R.T. Riley. 1989. Interaction of cyclopiazonic acid with rat skeletal muscle sarcoplasmic reticulum vesicles. Effect on Ca2+ binding and Ca2+ permeability. *Biochem. Pharmacol.* 38:3995–4003.

Gross, S.R., S.E. Mayer, and M.A. Longshore. 1976. Stimulation of glycogenolysis by beta adrenergic agonists in skeletal muscle of mice with the phosphorylase kinase deficiency mutation (I strain). *J. Pharmacol. Exp. Ther.* 198:526–538.

Hermann, H.P., O. Zeitz, B. Keweloh, G. Hasenfuss, and P.M. Janssen. 2000. Pyruvate potentiates inotropic effects of isoproterenol and Ca(2+) in rabbit cardiac muscle preparations. *Am. J. Physiol. Heart Circ. Physiol.* 279:H702–H708.

Kabbara, A.A., and D.G. Allen. 2001. The use of the indicator fluo-5N to measure sarcoplasmic reticulum calcium in single muscle fibres of the cane toad. *J. Physiol.* 534:87–97.

Korge, P., and K.B. Campbell. 1994. Local ATP regeneration is important for sarcoplasmic reticulum Ca2+ pump function. *Am. J. Physiol.* 267:C357–C366.

Kurebayashi, N., and Y. Ogawa. 2001. Depletion of Ca2+ in the sarcoplasmic reticulum stimulates Ca2+ entry into mouse skeletal muscle fibres. *J. Physiol.* 533:185–199.

Launikonis, B.S., J. Zhou, L. Royer, T.R. Shannon, G. Brum, and E. Rios. 2005. Confocal imaging of [Ca2+] in cellular organelles by SEER, Shifted Excitation and Emission Ratioing of fluorescence. *J. Physiol.* 567:523–543.

Lindemann, J.P., L.R. Jones, D.R. Hathaway, B.G. Henry, and A.M. Watanabe. 1983. beta-Adrenergic stimulation of phospholamban phosphorylation and Ca2+-ATPase activity in guinea pig ventricles. *J. Biol. Chem.* 258:464–471.

Nikolaev, V.O., M. Bunemann, L. Hein, A. Hannawacker, and M.J. Lohse. 2004. Novel single chain cAMP sensors for receptor-induced signal propagation. *J. Biol. Chem.* 279:37215–37218.

Palmer, A.E., C. Jin, J.C. Reed, and R.Y. Tsien. 2004. Bcl-2-mediated alterations in endoplasmic reticulum Ca2+ analyzed with an improved genetically encoded fluorescent sensor. *Proc. Natl. Acad. Sci. USA*. 101:17404–17409.

Posterino, G.S., and G.D. Lamb. 2003. Effect of sarcoplasmic reticulum Ca2+ content on action potential-induced Ca2+ release in rat skeletal muscle fibres. *J. Physiol.* 551:219–237.

Rios, E., and M.D. Stern. 1997. Calcium in close quarters: microdomain feedback in excitation-contraction coupling and other cell biological phenomena. *Annu. Rev. Biophys. Biomol. Struct.* 26:47–82.

Rudolf, R., M. Mongillo, P.J. Magalhaes, and T. Pozzan. 2004. In vivo monitoring of Ca^{2+} uptake into mitochondria of mouse skeletal muscle during contraction. *J. Cell Biol.* 166:527–536.

Sculptoreanu, A., T. Scheuer, and W.A. Catterall. 1993. Voltage-dependent potentiation of L-type Ca2+ channels due to phosphorylation by cAMP-dependent protein kinase. *Nature*. 364:240–243.

Shirokova, N., J. Garcia, G. Pizarro, and E. Rios. 1996. Ca^{2+} release from the sarcoplasmic reticulum compared in amphibian and mammalian skeletal muscle. *J. Gen. Physiol.* 107:1–18.

Shirokova, N., J. Garcia, and E. Rios. 1998. Local calcium release in mammalian skeletal muscle. *J. Physiol.* 512:377–384.

Somlyo, A.V., H.G. Gonzalez-Serratos, H. Shuman, G. McClellan, and A.P. Somlyo. 1981. Calcium release and ionic changes in the sarcoplasmic reticulum of tetanized muscle: an electron-probe study. *J. Cell Biol.* 90:577–594.

Sonnleitner, A., S. Fleischer, and H. Schindler. 1997. Gating of the skeletal calcium release channel by ATP is inhibited by protein phosphatase 1 but not by Mg2+. *Cell Calcium*. 21:283–290.

Tong, C.W., R.D. Gaffin, D.C. Zawieja, and M. Muthuchamy. 2004. Roles of phosphorylation of myosin binding protein-C and troponin I in mouse cardiac muscle twitch dynamics. *J. Physiol.* 558:927–941.

Vangheluwe, P., M. Schuermans, E. Zador, E. Waelkens, L. Raeymaekers, and F. Wuytack. 2005. Sarcolipin and phospholamban mRNA and protein expression in cardiac and skeletal muscle of different species. *Biochem. J.* 389:151–159.

Volpe, P., and B.J. Simon. 1991. The bulk of Ca2+ released to the myoplasm is free in the sarcoplasmic reticulum and does not unbind from calsequestrin. *FEBS Lett.* 278:274–278.

Yoshida, A., M. Takahashi, T. Imagawa, M. Shigekawa, H. Takisawa, and T. Nakamura. 1992. Phosphorylation of ryanodine receptors in rat myocytes during beta-adrenergic stimulation. *J. Biochem. (Tokyo)*. 111:186–190.

Zaccolo, M., and T. Pozzan. 2002. Discrete microdomains with high concentration of cAMP in stimulated rat neonatal cardiac myocytes. *Science*. 295:1711–1715.

Zhang, R., J. Zhao, A. Mandveno, and J.D. Potter. 1995. Cardiac troponin I phosphorylation increases the rate of cardiac muscle relaxation. *Circ. Res.* 76:1028–1035.

Rudolf et al., http://www.jcb.org/cgi/content/full/jcb.200601160/DC1

Supplemental text for Figure S1

To examine whether changes in $[Ca^{2+}]_{SR}$ in live muscle can be monitored with our probe, we tested its fluorescence changes during excitation–contraction coupling. Muscle contraction was elicited by applying electric pulses (5–50 Hz, for varying periods of time) to the exposed sciatic nerve using extracellular electrodes. Whole-fiber analysis of CFP and YFP fluorescence revealed an antiparallel behavior of the two chromophores during contraction; the intensity of CFP increases, whereas that of its xanthic counterpart decreases (Fig. S1 A). This indicates a drop in fluorescence resonance energy transfer, as would be expected after a decrease in $[Ca^{2+}]_{SR}$ (Zhang et al., 2002). The antiparallel behavior of the CFP and YFP signals was sometimes masked, usually when the total fluorescence intensity varied strongly, because of the vertical movement of the muscle fiber during contraction; however, the ratiometric data was not affected by these movement artifacts and correctly exhibited the drop in $[Ca^{2+}]_{SR}$. As shown in Fig. S1 B, the reduction in the mean $[Ca^{2+}]_{SR}$ along the fiber increased with higher stimulation frequency. As noted before using cytosolic or mitochondrially targeted cameleons (Rudolf et al., 2004), this apparent $[Ca^{2+}]_{SR}$ frequency correlation partially reflects the discrepancy between the durations of the measured Ca^{2+} transients and image acquisition; with <50 Hz (which causes tetanic contraction of the fibers), the muscle was contracted only part of the time necessary for the acquisition of a single image. Therefore, individual peaks of $[Ca^{2+}]_{SR}$ decrease were also measured with intermediate rises to baseline level. Upon averaging the whole image, the drop in ratio appeared less severe at 5 and 10 Hz than at 50 Hz.

To rule out contributions of fiber movement to the measured ratio changes, we undertook a series of controls. First, we tested the effect of changes in the focal plane on the YFP/CFP ratio by moving through the muscle fiber using the piezoelectric focus motor. This procedure did not lead to any observable ratio change (unpublished data). Next, we studied the effect of mechanically induced muscle deflection in the absence of any nerve stimulus on the ratiometric read-out. Therefore, D1ER-expressing muscles were monitored in situ with two-photon microscopy, as described in the legend for Fig. S1, and small mechanical impulses were applied to the object holder. As shown in Fig. S1 C (left), neither impulses from the frontal side nor from the lateral side of the object holder led to a change in YFP/CFP ratio, although in both cases a fiber deflection similar to the one observed upon nerve stimulation was clearly visible (gray columns). We then studied whether the contraction of the muscle itself could affect the ratiometric measurements. To this end, the muscles were slightly stretched during acquisition, without changing Ca^{2+} concentrations. This treatment resulted in fiber deflection, but not in any measurable YFP/CFP ratio change (Fig. S1 C, top right). Finally, we tested the ratiometric change of a non-Ca^{2+}–sensitive fluorescent PKA-based cAMP probe (Zaccolo and Pozzan, 2002) during nerve-induced muscle

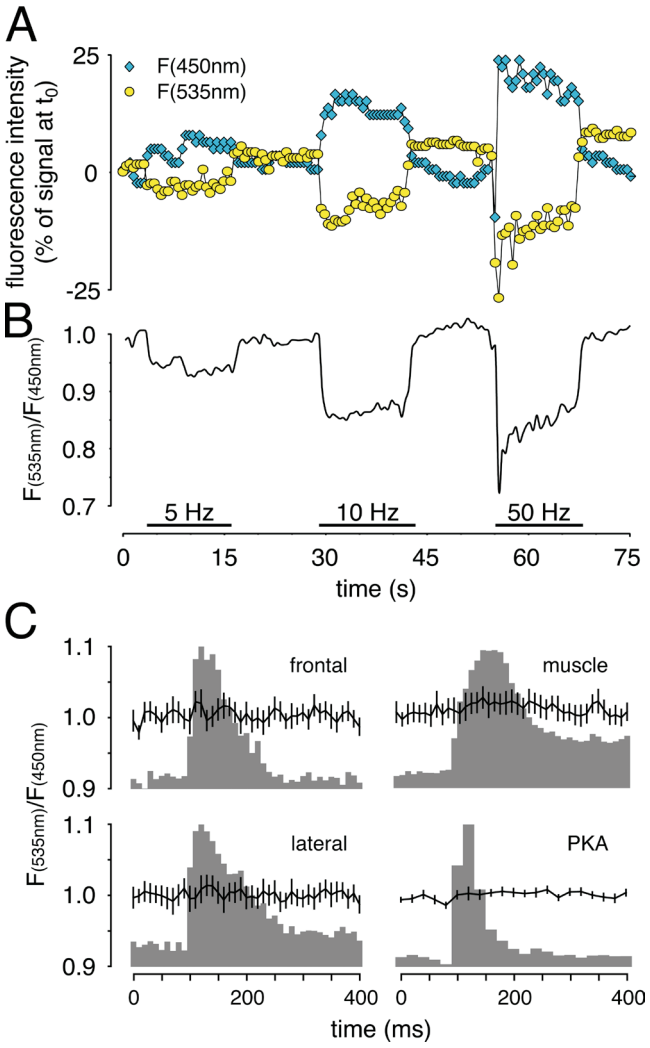

Figure S1. **D1ER reports reduction of $[Ca^{2+}]_{SR}$ upon stimulation of muscle contraction in situ and corrects for movements artifacts.** TA muscle was transfected with D1ER-based (A, B, and C [top left and bottom left]) or PKA-based cAMP probe–encoding cDNA (C, bottom right). (A and B) D1ER fluorescence was monitored by two-photon microscopy in situ during relaxation and contraction. Muscle contraction was induced at different stimulation frequencies, as indicated by the horizontal bars in B. (A) Individual traces of the fluorescence intensities at 450 ± 40 nm (CFP) and 535 ± 25 nm (YFP), as indicated. (B) YFP/CFP ratio corresponding to the traces in A; values normalized to the start of the experiment. (C) During two-photon microscopic monitoring, fiber deflection (gray columns) was elicited either by impulses on the front (frontal) or lateral side (lateral) of the object table, by slight stretching of the muscle itself (muscle), or by using nerve stimulation (PKA).

contraction. This probe has a striated pattern resembling that of D1ER, though it is clearly cytosolic. As depicted in Fig. S1 C (bottom right), this experiment also showed no appreciable change in YFP/CFP ratio, although fiber deflection was clearly observed. It should also be noted that under all conditions used, the fluorescence intensities of CFP and YFP changed in parallel upon fiber deflection, whereas in many fibers transfected with D1ER upon nerve-induced muscle contraction an antiparallel behavior of the two chromophores was observed, as shown in Fig. S1 A. Collectively, these results confirm the finding that the presented ratiometric measurements robustly corrected for gross movement artifacts.

Supplemental text for Figure S2

Ratiometric data were converted into $[Ca^{2+}]_{SR}$ values using the standard formula for cameleon probes (Arnaudeau et al., 2001; Miyawaki et al., 1997): $[Ca^{2+}]_{SR} = K_d([R - R_{min}]/[R_{max} - R])^{(1/n)}$, where K_d is the apparent dissociation constant, R is the YFP/CFP ratio, R_{min} is the YFP/CFP ratio in the presence of 1 mM CPA (a SERCA inhibitor), R_{max} is the maximal ratio observed in all examined fibers at rest, n is the Hill coefficient n_2 as described for D1ER (Palmer et al., 2004). Data is from six independent experiments.

Because a proper estimation of the K_d values of D1ER in vivo is practically unfeasible, we first referred to the in vitro calibration data published for D1ER (biphasic Ca^{2+} binding kinetics with K_d values of 0.81 and 69 μM, and Hill coefficients of 1.18 and 1.67 [Palmer et al., 2004]). For calibration of fluorescence data in terms of $[Ca^{2+}]$, R_{max} and R_{min} are also required. We tried to measure D1ER's R_{min} in situ by causing maximal $[Ca^{2+}]_{SR}$ depletion; we monitored tibialis anterior muscles in vivo before and after local application of high concentrations of CPA, followed by tetanic stimulation. Treatment of the muscle for 30 min with CPA (injected at 1 mM) reduced the resting YFP/CFP fluorescence ratio to 1.5 ± 0.11 (mean ± SEM; $n = 7$ fibers). Tetanic stimulation (50 Hz for 20 s) under these conditions resulted in no further drop of the fluorescence resonance energy transfer signal. We next addressed the determination of R_{max}. $[Ca^{2+}]_{SR}$ has been estimated to be in the millimolar range (Lamb et al., 2001; Somlyo et al., 1981; Volpe and Simon, 1991), so the cameleon probe should be saturated at such Ca^{2+} concentrations (Palmer et al., 2004). Thus, we initially assumed that the mean R measured in the relaxed state would be equal to R_{max}. This analysis, however, yielded a puzzling result because the basal YFP/CFP ratio ranged from ∼2.2 to ∼4, suggesting a great variability in the SR-loading state of the measured fibers. In these conditions, their mean value could hardly be presumed to indicate R_{max}. We then investigated whether a previously noted variability in YFP/CFP ratio drops during single twitches could be related to the differences in basal ratio. Interestingly, we found that an inverse linear relationship between basal YFP/CFP ratio and its decreases during contraction; moreover, the fibers with a basal ratio close to four hardly showed any ratio decrease upon contraction (Fig. S2 A), suggesting that this value is close to the maximum (i.e., the cameleon probe is saturated with Ca^{2+}). Consequently, we assumed this to be the R_{max} value.

The reason for such variability in basal YFP/CFP ratio values is not clear. It should be noted that the differences were larger between fibers from different animals than within any given animal. Because the TA muscle of rodents (although a fast muscle in general) contains fibers ranging from type I to type IIB (Staron et al., 1999), it cannot be excluded that in individual experiments different fiber subtypes were analyzed; alternatively, it may represent an animal-inherent variability. We consider that the fibers with lower YFP/CFP ratio cannot represent slow fibers because the duration of their contraction was always in the order of 100–150 ms. Because it is unlikely that upon CPA treatment the $[Ca^{2+}]_{SR}$ drops below 1 μM, we could discard the high affinity K_d of D1ER and assume a simple kinetic scheme with only one K_d at 69 μM. Based on these assumptions and the data shown in Fig. S2 A, the absolute values of $[Ca^{2+}]_{SR}$ and their drops during contraction were calculated and plotted (unpublished data). This revealed a surprisingly low mean basal $[Ca^{2+}]_{SR}$, ranging from ∼50–170 μM. An explanation for this phenomenon could be a change in the K_d for Ca^{2+} of the cameleon probe in situ because of the intra-SR environment, a process known to occur frequently with these indicators (Demaurex and Frieden, 2003; Filippin et al., 2003). Also, in the original description of D1ER, the $[Ca^{2+}]_{ER}$ values of cultured cells determined with this probe were ∼100 μM or even less, far below the values of 0.3–0.7 mM, typically measured in cultured cells with many other probes (Arnaudeau et al. , 2001, 2002; Kabbara and Allen, 2001; Pinton et al., 2000).

Thus, we sought to calculate the K_d for Ca^{2+} of D1ER in situ. To this end, we used a passive equilibration protocol, as previously described (Filippin et al., 2003). We first tried to use single muscle fibers isolated from the transfected muscles, but in our hands the recovery of healthy transfected fibers was extremely low, and their use for calibration purposes was impractical. Thus, we turned to cell lines, HeLa and CHO cells, which were transiently transfected with D1ER. Fig. S2 B depicts a typical YFP/CFP ratio trace of the calibration experiments for which we used the following protocol: first, cells were stimulated with 100 μM histamine and the SERCA pumps were blocked with 5 μM thapsigargin, resulting in a rapid and massive drop of $[Ca^{2+}]_{ER}$ (Fig. S2 B, a); the cells were then permeabilized with 100 μM digitonin in an intracellular-like medium (140 mM KCl, 10 mM NaCl, 1 mM $MgCl_2$, 20 mM Hepes, pH 7.0) without ATP (Fig. S2 B, b) and supplemented with 200 μM EGTA. Another small drop in $[Ca^{2+}]_{SR}$ occurred (Fig. S2 B, c). Given that the SERCA are blocked by thapsigargin and that no ATP was present in the medium, we assumed that the $[Ca^{2+}]_{SR}$ should have dropped to ∼1 μM and, thus, we considered the YFP/CFP ratio under these conditions as the R_{min} value. Finally, the perfusing medium was supplemented with $CaCl_2$ concentrations ranging from 0 to 10 mM Ca^{2+} (to reach the R_{max} value; Fig. S2 B, d–i). At each step increase of the $[Ca^{2+}]$ in the medium, a rise in the YFP/CFP ratio occurred that stabilized within 1–2 min. When the $CaCl_2$ concentration in the medium was increased >5–10 mM, no further increase in the YFP/CFP ratio was observed and we assumed this value as R_{max}. As shown in Fig. S2 C for HeLa cells, assuming complete equilibration between extracellular and ER $[Ca^{2+}]$, this calibration resulted in an apparent K_d of ∼220 μM for D1ER in situ, i.e., about three times as high as that obtained in vitro (Palmer et al., 2004). To verify, whether the used calibration procedure indeed led to an equilibration between the extracellular

and ER $[Ca^{2+}]$, we monitored the $[Ca^{2+}]_{ER}$ using the same protocol in HeLa cells expressing ER-targeted, low Ca^{2+} affinity, aequorin reconstituted with coelenterazine n, as previously described (Pinton et al., 2000). Using this probe, we found that at extracellular $[Ca^{2+}]$ up to 1 mM the medium and ER $[Ca^{2+}]$ were practically identical, whereas at higher extracellular $[Ca^{2+}]$ further $[Ca^{2+}]_{ER}$ rises were marginal (unpublished data). The K_d for Ca^{2+} of D1ER based on the values of $[Ca^{2+}]_{ER}$ measured with aequorin was 200 μM. We used this value for all following calculations. The $[Ca^{2+}]_{ER}$ of intact HeLa and CHO cells at rest was calculated to be ~350 μM, i.e., which is very similar to that measured by other approaches (Pinton et al., 2000). As shown in Fig. S2 D, assuming a K_d of 200 μM, the basal $[Ca^{2+}]_{SR}$ in the TA muscle fibers in vivo was found to be 308 ± 30 μM, and the drop during single twitches was 53 ± 6 μM (mean ± SEM for both; $n = 18$ fibers). We cannot exclude that a further drift in the K_d of D1ER may occur within the lumen of the SR in TA fibers. If this were the case, the reported values of $[Ca^{2+}]_{SR}$ would be underestimated.

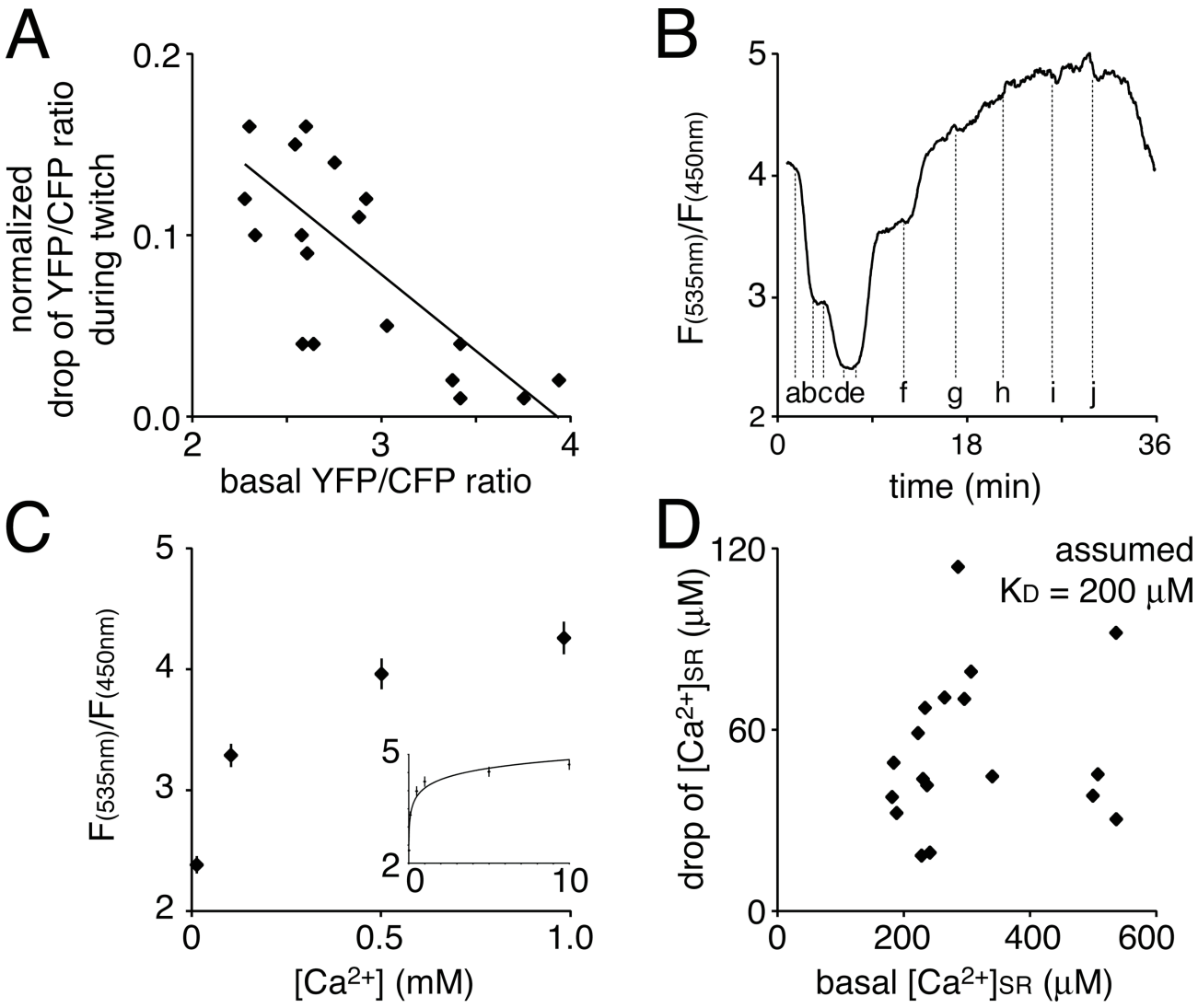

Figure S2. **Calibration of D1ER and correlation between the $[Ca^{2+}]_{SR}$ loading status and Ca^{2+} release.** TA muscle (A and D) or HeLa cells (B and C) were transfected with cDNA coding for D1ER. Cameleon fluorescence signals were monitored with two-photon microscopy in situ during contraction at a frequency of 1 Hz (A and D) or with conventional video fluorescence microscopy using the calibration protocol described above (B and C). (A) Graph showing the drop in YFP/CFP ratio during single twitches (normalized to the basal ratio of the same fiber) as a function of the basal YFP/CFP ratio. For each point, the values from 25 individual twitches of one single fiber were averaged. Data are from 18 fibers (six experiments). (B) Typical YFP/CFP ratio trace of a calibration experiment. Dotted lines indicate treatments: a, 100 μM histamine plus 5 μM thapsigargin; b, 100 μM digitonin; c, 200 μM EGTA; d, ~2 μM $CaCl_2$; e, 0.1 mM $CaCl_2$; f, 0.5 mM $CaCl_2$; g, 1 mM $CaCl_2$; h, 5 mM $CaCl_2$; i, 10 mM $CaCl_2$; j, 200 μM EGTA. (C) Measured YFP/CFP ratio as a function of $[Ca^{2+}]$ in the bath solution. Data from the same data set are shown at two different scales (i.e. 0–1 mM for the large graph; 0–10 mM for the inset graph). (D) Correlation between basal $[Ca^{2+}]_{SR}$ and the drop in $[Ca^{2+}]_{SR}$ during single twitches, based on the data shown in A, R_{min} and R_{max} as indicated in the text and an assumed K_d of 200 μM.

Supplemental materials and methods

Expression plasmids and chemicals

Transfection experiments used the following constructs in pcDNA3 (Invitrogen): ER-AEQ (Pinton et al., 2000), RII-CFP, and C-Venus (Zaccolo and Pozzan, 2002).

Tissue culture

HeLa and CHO cells were cultured using DME containing 10% horse serum at 37°C and 5% CO_2. Transient transfection was performed using a standard protocol with Fugene 6 transfection reagent (Roche).

References

Arnaudeau, S., M. Frieden, K. Nakamura, C. Castelbou, M. Michalak, and N. Demaurex. 2002. Calreticulin differentially modulates calcium uptake and release in the endoplasmic reticulum and mitochondria. *J. Biol. Chem.* 277:46696–46705.

Arnaudeau, S., W.L. Kelley, J.V. Walsh Jr., and N. Demaurex. 2001. Mitochondria recycle Ca(2+) to the endoplasmic reticulum and prevent the depletion of neighboring endoplasmic reticulum regions. *J. Biol. Chem.* 276:29430–29439.

Demaurex, N., and M. Frieden. 2003. Measurements of the free luminal ER Ca(2+) concentration with targeted "cameleon" fluorescent proteins. *Cell Calcium*. 34:109–119.

Filippin, L., P.J. Magalhaes, G. Di Benedetto, M. Colella, and T. Pozzan. 2003. Stable interactions between mitochondria and endoplasmic reticulum allow rapid accumulation of calcium in a subpopulation of mitochondria. *J. Biol. Chem.* 278:39224–39234.

Lamb, G.D., M.A. Cellini, and D.G. Stephenson. 2001. Different Ca2+ releasing action of caffeine and depolarisation in skeletal muscle fibres of the rat. *J. Physiol.* 531:715–728.

Miyawaki, A., J. Llopis, R. Heim, J.M. McCaffery, J.A. Adams, M. Ikura, and R.Y. Tsien. 1997. Fluorescent indicators for Ca2+ based on green fluorescent proteins and calmodulin. *Nature*. 388:882–887.

Pinton, P., D. Ferrari, P. Magalhaes, K. Schulze-Osthoff, F. Di Virgilio, T. Pozzan, and R. Rizzuto. 2000. Reduced loading of intracellular Ca^{2+} stores and downregulation of capacitative Ca^{2+} influx in Bcl-2–overexpressing cells. *J. Cell Biol.* 148:857–862.

Staron, R.S., W.J. Kraemer, R.S. Hikida, A.C. Fry, J.D. Murray, and G.E. Campos. 1999. Fiber type composition of four hindlimb muscles of adult Fisher 344 rats. *Histochem. Cell Biol.* 111:117–123.

Zhang, J., R.E. Campbell, A.Y. Ting, and R.Y. Tsien. 2002. Creating new fluorescent probes for cell biology. *Nat. Rev. Mol. Cell Biol.* 3:906–918.